Monthly Mean Wind Stress and Sverdrup Transports in the North Atlantic: A Comparison of the Hellerman–Rosenstein and Isemer–Hasse Climatologies

CLAUS W. BÖNING, RALF DÖSCHER AND HANS-JÖRG ISEMER

Institut für Meereskunde, Kiel, F.R.G.

(Manuscript received 26 March 1990, in final form 3 August 1990)

ABSTRACT

The monthly mean wind stress climatology of Hellerman and Rosenstein (HR) is compared with the climatology of Isemer and Hasse (IH), which represents a version of the Bunker atlas (BU) for the North Atlantic based on revised parameterizations. The drag coefficients adopted by IH are 21% smaller than the values of BU and HR, and the calculation of wind speed from marine estimates of Beaufort force (Bft) is based on a revised Beaufort equivalent scale similar to the scientific scale recommended by WMO. The latter choice significantly increases wind speed below Bft 8, and effectively counteracts the reduction of the drag coefficients.

Comparing the IH stresses with HR reveals substantially enhanced magnitudes in the trade wind region throughout the year. At 15°N the mean easterly stress increases from about 0.9 (HR) to about 1.2 dyn cm^{-2} (IH). Annual mean differences are smaller in the region of the westerlies. In winter, the effect due to the reduced drag coefficient dominates and leads to smaller stress values in IH; during summer season the revision of the Beaufort equivalents is more effective and leads to increased stresses.

Implications of the different wind stress climatologies for forcing the large-scale ocean circulation are discussed by means of the Sverdrup transport streamfunction (ψ_S): Throughout the subtropical gyre a significant intensification of ψ_S takes place with IH. At 27° N, differences of more than 10 Sv (1 Sv $\equiv 10^6$ m^3 s^{-1}) are found near the western boundary. Differences in the seasonality of ψ_S are more pronounced in near-equatorial regions where IH increase the amplitude of the annual cycle by about 50%. An eddy-resolving model of the North Atlantic circulation is used to examine the effect of the different wind stresses on the seasonal cycle of the Florida Current. The transport predicted by the numerical model is in much better agreement with observations when the circulation is forced by IH than by HR, regarding both the annual mean (29.1 Sv vs 23.2 Sv) and the seasonal range (6.3 Sv vs 3.4 Sv).

1. Introduction

An important element of the coupling between atmosphere and ocean is the surface momentum flux, or wind stress, by which atmospheric winds drive oceanic currents. In recent years, several authors have derived monthly mean wind stress fields based on surface marine datasets.

Estimates of the surface wind stress $\vec{\tau} = (\tau^x, \tau^y)$ are most commonly based on the bulk aerodynamic formula

$$\vec{\tau} = \rho_A c_D |\mathbf{U}| \mathbf{U} \qquad (1)$$

where ρ_A is the density of air at the surface, c_D the drag coefficient, and $\vec{\tau}$ is assumed to be parallel to the wind speed $\mathbf{U} = (u, v)$. There are several sources of error in estimating the wind stress: an uncertainty arising from poor sampling or inadequate spatial resolution of the wind data, possible systematic errors in estimating the wind speed from ship observations, and the choice of a value for the drag coefficient c_D.

Earlier estimates of climatological $\vec{\tau}$ fields had been based on wind rose data, i.e., statistical information about the wind distribution over the world ocean (e.g., Hellerman 1967). A major contribution is due to Bunker (1976, hereafter BU) who made use of the individual observations of the Voluntary Observing Fleet collected by the National Climatic Center in the marine surface dataset (TDF-11). As part of an effort to estimate the total energy exchange between ocean and atmosphere, Bunker computed monthly mean wind stress distributions for the North Atlantic Ocean. The period considered was 1941–72, and the values were collected for irregularly shaped areas, ranging from 1° × 1° near shore to typically 2° × 5° in open ocean. Bunker used a drag coefficient depending on wind speed $U = |\mathbf{U}|$ and atmospheric stability. The equivalent neutral drag coefficient c_{DN} was chosen according to observational and theoretical results available to Bunker at that time (see Fig. 2).

A calculation of monthly mean wind stress fields for 2° × 2° boxes over the World Ocean was performed by Hellerman and Rosenstein (1983, hereafter HR), based on the surface marine dataset for the period 1870–1976. They essentially applied the same parameterizations as BU. The HR climatology has found a wide distribution in the oceanographic modeling community and has become the standard dataset for

Corresponding author address: Dr. Claus Boning, Institut fur Meereskunde, Dusternbrooker Weg 20, D-2300 Kiel 1, FRG.

the specification of the dynamic boundary condition in large-scale ocean circulation models.

More recent observational and theoretical results on c_D values under open sea conditions indicated that Bunker's values were possibly too high (e.g., Smith 1980; Large and Pond 1981). Harrison (1989) presented a new calculation of global monthly mean stresses based on a similar dataset as the one used by HR but employing the c_D formulation given by Large and Pond (1981) (see Fig. 2). Since these coefficients are smaller by about 20%, Harrison's stresses are almost everywhere smaller than those of HR.

Another source of possible systematic error in estimating wind stress had not received a similar attention yet (Cardone et al. 1990; Isemer and Hasse 1990). Historical marine wind reports are usually based on estimates of Beaufort numbers rather than anemometer measurements (e.g., Quayle 1980). Wind speed as given in the marine data decks is obtained by converting Beaufort estimates to wind speed by use of the official WMO scale. It has been pointed out by several authors (WMO 1970; Kaufeld 1981) that this scale systematically underestimates wind speeds below Beaufort 8, and overestimates above. The Commission of Marine Meteorological Affairs recommended the use of a revised Beaufort equivalent for scientific purposes (WMO 1970).

Recently, Isemer and Hasse (1987, hereafter IH) presented a new climatology of air–sea fluxes for the North Atlantic Ocean. The calculations are based on the original dataset of Bunker, but revised parameterizations were used both for the drag coefficient c_D and the Beaufort equivalents. In contrast to the stress calculation of Harrison (1989), the reduction of the stress values due to the altered drag coefficients is effectively counteracted in IH by the simultaneous revision of the Beaufort equivalents.

In this paper we will present a comparison of the IH and HR wind stress climatologies for the North Atlantic Ocean. Our particular attention is directed at those properties of the monthly mean stress fields which are most relevant for the forcing of the large-scale ocean circulation.

A major effort in modeling ocean circulation had been initiated recently in anticipation of the modeling needs of the World Ocean Circulation Experiment (WOCE). As the first step of a WOCE "community modeling effort" an eddy-resolving model of the wind driven and thermohaline circulation has been developed (Bryan and Holland 1989) aimed at a simulation of the hydrographic structure and its variability of the North Atlantic Ocean. We use this high resolution model to examine the impact of the different wind stress climatologies on the volume transport in the subtropical North Atlantic. In this paper we shall only present results for the transport through the Straits of Florida where a well-established observational picture can provide a stringent test for models of large-scale circulation. A more thorough examination of numerical model results for the seasonal variation of the western boundary current system is presented separately (Böning et al. 1990).

The paper is organized as follows. In section 2 we will review in some more detail the databases and parameterizations adopted by HR and IH. The different parameter choices lead to characteristic differences in the wind stress fields which will be described in section 3. This is followed by a comparison of the Sverdrup transports (section 4) that would be anticipated by applying simple ocean circulation theory. In section 5 the relevance of these properties for the wind-driven ocean circulation is discussed; in particular, the annual cycle of the mass transport through the Florida Straits as predicted by the high resolution Atlantic model is shown and compared with observations.

2. Data and parameterizations used by HR and IH

As both climatologies are influenced by the pioneering work of Bunker (1976) we start summarizing the main features of the BU dataset.

a. Bunker

Bunker (1976) derived long term monthly averages of both basic meteorological variables and derived air–sea interaction fluxes for irregularly spaced "gerrymanders" in the North Atlantic Ocean. He used 8 million individual ship observations from the period 1941–72 archived by the National Climatic Centre (NCC). For computation of climatological means of the east- and north component of $\vec{\tau}$, BU used the "individual" rather than the "climatological" method: τ^x and τ^y were calculated from each individual ship observation, and these individual estimates were averaged afterwards, thus preserving the cross correlations between the parameters involved. Hence, if the overbars denote averaging in time and space, $\overline{\tau_i^{x,y}}$ is obtained from

$$\overline{\tau_i^{x,y}} = \overline{\rho_A c_D |\mathbf{U}| U^{x,y}} \tag{2}$$

where the index i denotes the individual method, in contrast to the climatological method, index c

$$\overline{\tau_c^{x,y}} = \overline{\rho_A c_D} \, \overline{|\mathbf{U}|} \, \overline{U^{x,y}}. \tag{3}$$

From a publication by Quayle (1980, his Fig. 23) it can be deduced that more than 90% of the marine wind reports in the NCC data archives of the period BU used are based on wind estimates rather than anemometer measurements. These estimates are transformed to surface wind speed by means of the official Beaufort equivalent scale of World Meteorological Organization (WMO).

Values of the drag coefficients c_D under neutral conditions were chosen by BU according to experimental and theoretical results published until 1972. To incorporate the stability dependence of c_D as a function of

air–sea temperature differences, ΔT, BU applied ratios of drag coefficients under non-neutral conditions to their neutral values which have been published by Deardorff (1968). Bunker established a table of c_D for wind speed intervals of 5 m s^{-1} and variable intervals of ΔT.

b. HR

In an effort to get a consistent wind stress dataset for the whole World Ocean, HR applied a polynomial fit of BU's c_D-values to more than 35 million marine wind observations from the period 1870–1976. Long-term monthly averages were defined on a regular 2° grid net over the World Ocean. A comparison of BU's and HR's stresses in the North Atlantic Ocean show that due to a more restrictive smoothing procedure applied by HR the extrema of their stress components tend to be smaller than those of BU. In general, however, there is good agreement between both climatologies for the North Atlantic Ocean. Hence, the climatology of HR can be regarded as an extension of BU's work without changing basic parameterizations: 1) extension to more data over a longer period, 2) extension to the whole World Ocean, and 3) definition on a regular grid net suitable for numerical computer calculations. HR adopted BU's principle procedures; the "individual" method in connection with BU's coefficients were used. In both climatologies, wind speeds are taken as given in the data archives, i.e., decoded by the official Beaufort scale of WMO.

c. IH

The IH-climatology uses part of the BU dataset but incorporates three basic differences to both BU and HR: 1) a revised Beaufort equivalent scale is used to decode wind estimates, 2) reduced drag coefficients are applied, and 3) the influence of humidity on the stability of the atmospheric surface layer is considered. In the following we summarize aspects of the three changes separately.

1) BEAUFORT EQUIVALENT SCALE

It is only the last 20–30 years that a significant fraction of the wind reports in marine datasets consists of anenometer measurements. The overwhelming contribution up to, about 1970 is due to wind estimates expressed in Beaufort numbers which have to be converted to wind speed by means of a Beaufort equivalent scale. For all climatologies (except the Atlantic Ocean portion of the Historical Sea Surface Temperature (HSST) dataset, see Coads 1985) so far known to these authors the official scale of WMO, code 1100 (WMO 1970), has been used, including BU and HR. Also the Coads dataset (see Coads 1985) uses the old WMO scale. It is known (WMO 1970) that this scale exhibits significant systematic errors. Although the Commission of Marine Meteorology Affairs (CMM) strongly suggested introducing revised Beaufort equivalents, WMO still uses the old scale for routine Weather Service (WMO 1970). For scientific purpose, however, a revised scientific scale was suggested by CMM.

Following the recommendation by CMM, IH use a recently revised Beaufort scale published by Kaufeld (1981) which is very similar to the scientific scale (often called CMM IV Beaufort scale) suggested by CMM. Quite recently, Cardone et al. (1990) investigated the effect of their own, revised equivalent scale on trends in wind anomalies since World War II. Although the database used for calibration of their scale is smaller than that of Kaufeld's, both scales are very similar and differ significantly from the old scale. These differences to the official WMO scale are considerable (Fig. 1a): Individual wind speeds are increased for Beaufort numbers less and equal than 7, up to a factor of 2, and are reduced slightly for estimates of more than Beaufort

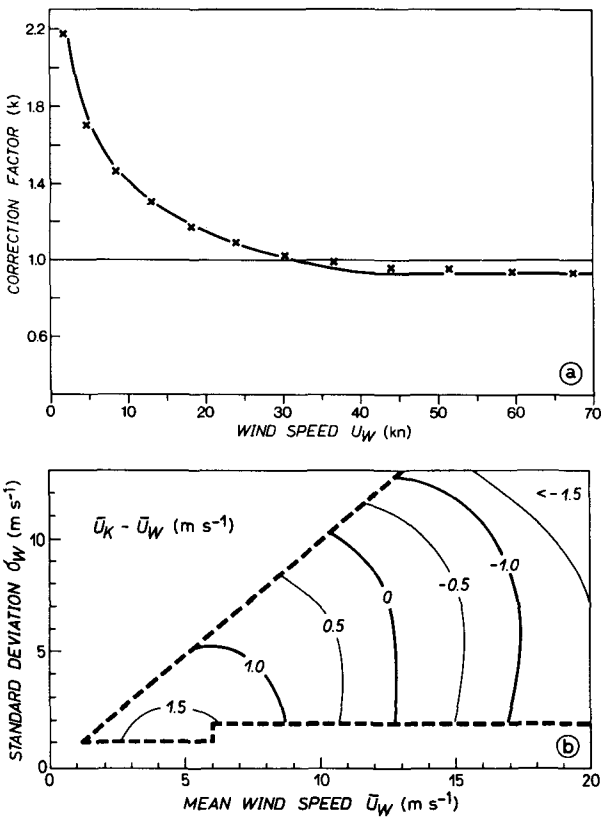

FIG. 1. (a) The correction factor $k(U_w)$ as a function of wind speed U_w (in km), decoded according to the official WMO scale. Multiplying individual observations of U_w with $k(U_w)$ results in wind speeds U_k transformed according to the scientific scale of Kaufeld (1981) for a nominal reference height of 25 m. Note that $k(U_w)$ may only be applied to individual observations (adopted from Isemer and Hasse 1987). (b) Theoretically predicted difference between monthly averages of wind speed, $\bar{U}_K - \bar{U}_W$ (in m s^{-1}), as a function of the monthly mean, $\bar{U}_W$, and the standard deviation of U_W, σ_w. For this comparison a nominal reference height of 10 m is used for both wind speeds.

7. Note, that the correction function is nonlinear in wind speed and hence may not be applied to averages of U. IH fitted a two-parameter Weibull distribution to means and standard deviations of U available from the BU dataset, applied the correction $K(U_w)$ (the index w denotes transformation by the WMO scale) and calculated new means $\overline{U_K}$ and standard deviations (the index K denotes transformation by the Kaufeld-scale) for the North Atlantic Ocean. Theoretically predicted differences $\overline{U_K} - \overline{U_w}$ (Fig. 1b) for real wind statistics may exceed 1.5 m s^{-1}. (Note that for the comparison in Fig. 1b the difference between the reference level of Kaufeld's scale and the WMO scale has been taken into account.) In the North Atlantic Ocean differences in mean monthly wind speed vary between 0 to 0.3 m s^{-1} in the west wind drift in January and more than 1.4 m s^{-1} in the trade wind region throughout the year. Related to the old wind climatologies this corresponds to an increase of mean speed up to 5% (in winter) and 20% (in summer) in the westerlies. In tropical latitudes the increase is between 20% and 30% throughout the year.

Methods and effects of the application of the revised scale are described in detail by Isemer and Hasse (1990). Effects on estimates of air–sea interaction fluxes are substantial. They calculate the effect of the revised scale on zonally averaged monthly means of the wind stress to be between 10 and 20% in the west wind drift and up to 45% in the trade wind region of the North Atlantic.

2) Drag coefficients

Since the publication of BU's coefficient results of a number of well performed open ocean experiments especially under long fetch conditions (e.g., ATEX, NORPAX, AMTEX, GATE, JASIN, measurements at the BIO tower) have been published. Based on a collection of these experimental results (e.g., Hasse et al. 1978; Smith 1980; Large and Pond 1981) IH reduced BU's coefficients by 21% for all wind speed and stability categories. For computational reasons a constant correction factor was used. Hence, the somewhat unphysical step function dependence of c_D as a function of wind speed introduced by Bunker remained. The reduction was determined by taking ratios between BU's choice and the newer experimental values for different wind speed ranges and averaging the resulting correction factors. Although IH's choice of experimental results comprises the most elaborate measurements (which are mainly obtained by the eddy correlation technique) and data evaluations, the scatter in the results for c_D is considerable (up to 30%). The effects on bulk derived surface fluxes due to the use of different coefficient schemes has been demonstrated by Blanc (1985) with meteorological data from Ocean Weather Ship C. The resulting uncertainties in derived air–sea fluxes appeared unacceptably large. Hence, instead of picking out one specific result IH preferred to use coefficients lying well within the uncertainty range of the collection of open ocean measurements. Bunker's values are systematically higher on average by the percentage amount mentioned.

Recently, a workshop on atmospheric forcing of ocean circulation recommended that ocean modelers should adopt a particular set of bulk coefficients and continue to use them for a number of years (Scoggins and Moers 1988). For c_D the experimental results of Smith (1980) (referenced S henceforth) were recommended by the workshop mentioned. Harrison (1989) adopted the values of Large and Pond (1981) (LP) which also seem to be preferred in the context of WOCE modeling efforts (e.g., see Oberhuber 1988). We compare drag coefficients representative for different stability conditions in Fig. 2. The results of both LP and S match fairly well with the values used by IH for both neutral and non-neutral conditions. For some combinations of U and ΔT the IH values tend to be slightly higher than those of LP and S. However, the net effect on climatological averages of $\vec{\tau}$ is about or less than 5% which is of order, or even smaller, than the difference between the experimental results of LP and S.

Beaufort estimates after World War II are exclusively based on visual impressions of the state of the sea surface. Hence, these estimates are physically closer related to the vertical flux of momentum, i.e., wind stress, than to wind speed in a specific reference height. Assuming that the calibration of the revised equivalent scale was performed under neutral conditions (and having in mind the dependence of the logarithmic wind profile for different stability categories) an estimate made in stable (unstable) density stratification would yield a too low (high) equivalent wind speed for a given reference height. Resulting wind stresses then would be too low (high), the bias being reinforced by the stability dependent drag coefficient. Kaufeld (1981) did not mention any correction depending on stratification when calibrating his scale. It is difficult to estimate the effect of stratification in his dataset (observations on six ocean weather ships and voluntary observing ships from more than 20 years). His scale will presumably represent slightly to moderately unstable conditions rather than neutral or even stable ones. Hence, for the long term average one should expect that the wind stress data in IH (but also in other compilations) tend to be overestimated in strongly unstable conditions (e.g., Gulf Stream region) and underestimated in regions with stable conditions (e.g., upwelling regions). However, a quantitative estimate of this bias, if any, is still an unresolved issue.

3) Influence of surface layer humidity

The vertical density gradient determines the static stability in the surface layer over the ocean. Hence, as

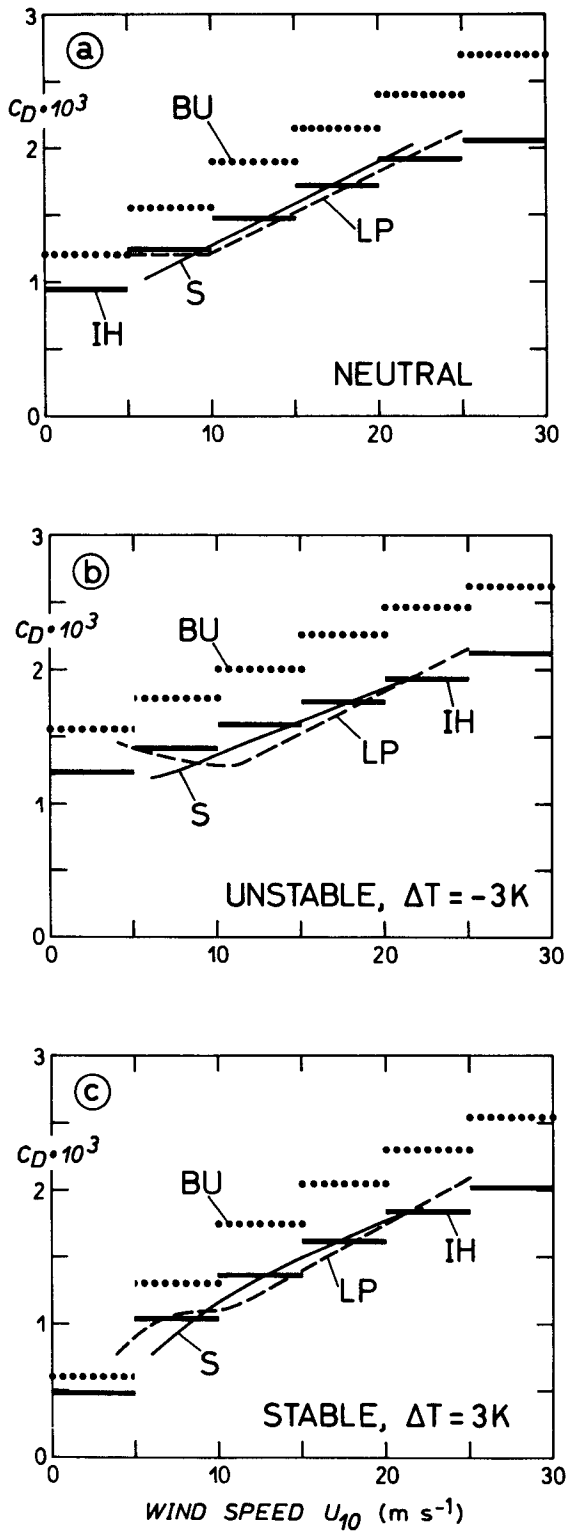

FIG. 2. The drag coefficient c_D as a function of wind speed U_{10} for the reference height of 10 m for (a) neutral, (b) unstable, and (c) stable density stratification. Displayed are the forms used by Bunker (1976), BU, Isemer and Hasse (1987), IH, as well as the experimental results published by Smith (1980), S, and Large and Pond (1981), LP.

is done in all experimental work, IH consider the surface layer humidity lapse profile over sea for the calculation of the stability dependence of the drag coefficients using the virtual temperature difference instead of the air–sea temperature difference as the indicator for atmospheric stability. The resultant density stratification is more unstable than if determined by the air–sea temperature difference, increasing the drag coefficient. However, the effect on averages of $\vec{\tau}$ is an order of magnitude smaller than the effect resulting from the revision of Beaufort equivalents and drag coefficients.

In summary, two effects will cause the main differences between the wind stress climatologies of HR (or BU) and IH. The reduction of 21% by the use of drag coefficients in accordance with recent experimental evidence is counteracted, or, as in most climate regions and months, overcompensated by the increase due to the application of a more realistic surface wind speed climatology.

d. Computational aspects

Isemer and Hasse (1987) used the meteorological mean BU dataset to recalculate $\tau^{x,y}$. In order to retain the cross correlations but accommodate the necessary changes discussed above, local correction factors expressing the difference between the results obtained by the individual method and those obtained by the climatological method were calculated from the original BU dataset for τ^x and τ^y in each gerrymander and month. The mean monthly value of $|\vec{\tau}|$ was calculated then from the mean revised wind speed and the corrected drag coefficients. In order to obtain the vector-averaged wind, IH assumed that the directional steadiness does not change when applying other than the WMO scale. Furthermore, in order to decompose monthly averages of $|\vec{\tau}|$ into τ^x and τ^y IH assumed no change in mean monthly wind direction. The resulting monthly components of τ^x and τ^y were then multiplied by the local correction factors in order to include the cross correlations. Annual averages of τ^x and τ^y were obtained by averaging the respective monthly means. Hence, significant differences in stress direction can be expected to occur only in the annual mean, and not in maps for individual months (see Isemer and Hasse 1990 for more details).

In order to apply the drag coefficients for the 10 m reference height, IH transformed the revised wind statistics to a 10 m level using the neutral logarithmic wind profile. The drag coefficient used for computing the mean stress was taken as a function of the revised mean wind speed; hence an interaction between the corrected coefficients and the revised wind is allowed for, at least in the mean. The IH climatology is available on a regular 1° grid net. To facilitate comparison, the HR climatology (which is given on 2° × 2° boxes) was interpolated on to a regular 1° grid net. All fields shown in this paper are derived from the wind stress

data given on this net. No smoothing of these fields was applied prior to calculation of curl$\vec{\tau}$ or Sverdrup transports, respectively.

There is one important deviation from the original IH atlas we had to make in order to apply this dataset to the high resolution Atlantic model. Since the model includes equatorial dynamics and has its southern boundary at 15°S, and the IH fields are confined to the Northern Hemisphere, we had to blend the IH stresses with HR south of the equator. In order to avoid unphysically large gradients at the equator, a transition region between the equator and 5°N was introduced in which a weighted average between both fields was used. In the following we will discuss the differences between HR and IH north of 5°N.

3. Annual cycle of wind stress

Figure 3 shows the annual mean wind stress of both climatologies and the vector differences (IH minus HR). The main feature of the stress distribution standing out is the anticyclonic gyre associated with the subtropical high pressure cell centered at about 30°N, 30°W. The major differences between the fields are a substantially enhanced magnitude of the IH stresses in the trade wind region, an enhanced northward stress in the northwest Atlantic, and a spatial structure with smaller scales and stronger extremas than in HR north of 60°N. The latter feature can be regarded as an effect of the different spatial sampling and smoothing procedures adopted by HR and IH (i.e., Bunker), respectively, in an area of poor data coverage. A similar difference between their fields and the original wind stresses of Bunker was already noted by HR. Except for these northern areas, the wind stress differences can be explained as a result of the different parameterization schemes used. In the trade wind region, the effect of the revised Beaufort equivalent dominates the effect due to the reduction of the drag coefficient throughout the year and leads to enhanced stresses without much directional change.

The increased magnitude of the annual mean northward stress in the region of the westerlies represents a combined effect of the speed dependence of the multiplication factor $k(U)$ and the strong annual cycle of the stress field (e.g., see Isemer and Hasse 1987 for the distribution of monthly mean stresses over the year). In winter, when the westerlies are strongest, the effect of the revised c_D dominates and leads to a reduction of wind stress between 40° and 50°N. In summer, the subtropical high greatly expands toward the north, leading to a more southerly wind direction in the northwest Atlantic. In this season the influence of the Beaufort equivalent is more important and leads to increased IH stresses. The differences between stress values of IH and HR during the summer season are reflected as a directional change in the annual mean fields.

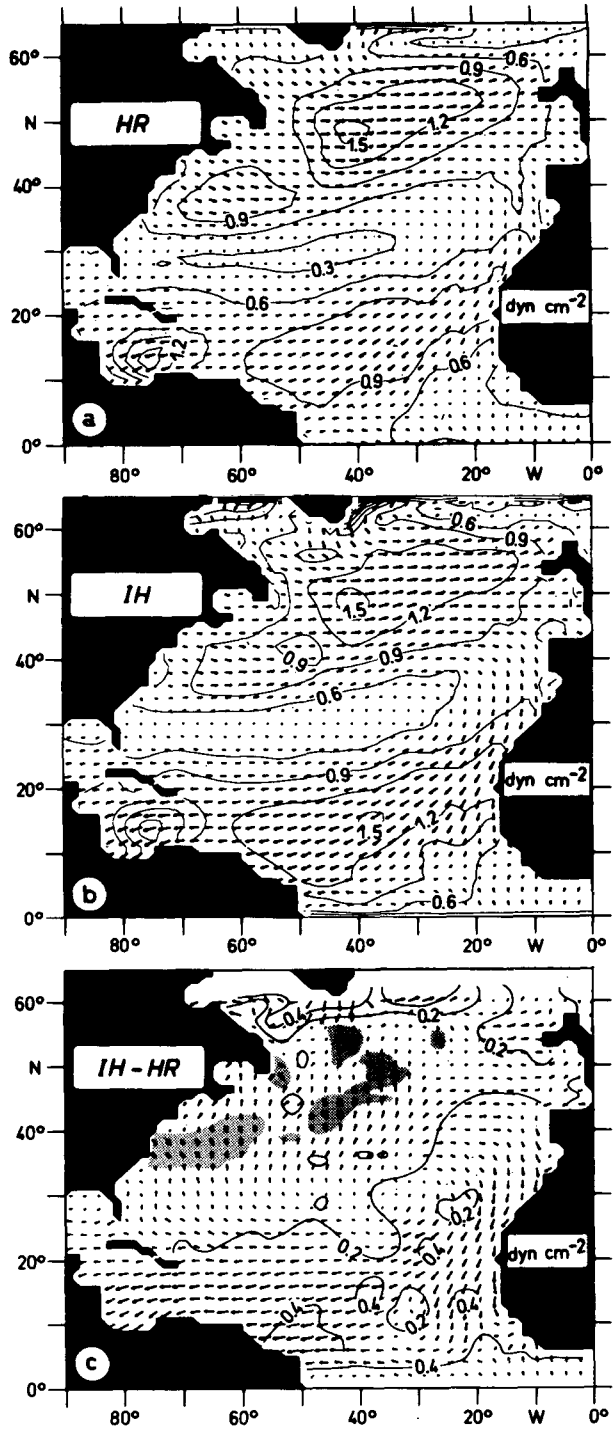

FIG. 3. Annual mean wind stress for the North Atlantic Ocean: (a) HR, (b) IH. The contour lines delineate the magnitude of the stress with an interval of 0.3 dyn cm^{-2}. In (c) the vector difference, IH minus HR, is displayed; the contour interval is 0.2 dyn cm^{-2}. The stippling indicates negative values

The seasonality of the stresses can be visualized more easily by concentrating on the latitudinal dependence only. Figure 4 shows latitude–time sections of the wind

stress components, zonally averaged over the width of the North Atlantic. The average operator will be denoted by $[\cdot]_\lambda$. Both climatologies exhibit a strong annual cycle of wind stress magnitude in the subpolar region. Over most of the winter season the westerly wind stress of IH is less than HR (the biggest difference is about -0.3 dyn cm^{-2} at 45°N in February). Both fields reach similar maxima though with >1.8 dyn cm^{-2} in December around 52°N. In summer and early fall the IH stresses are stronger ($+0.4$ dyn cm^{-2} at 50°N in September).

The seasonality of the northeast trades is not only influenced by the meridional extension of the Azores high, but also the migration of the intertropical convergence zone. Both effects lead to a weak semiannual cycle of the stresses around 15°N. The first causes a winter maximum of easterly stress ($[\tau^x]_\lambda < -1.2$ dyn cm^{-2} in IH, and <1.0 dyn cm^{-2} in HR), whereas the northward shift of the ITCZ in summer is associated with a secondary maximum in June–July.

The position of the ITCZ is reflected in the zero contour of $[\tau^y]_\lambda$. It reaches its northernmost position in August. At this time a strong difference between IH and HR can be identified with respect to the magnitude of the southeast trades. At 5°N the southerly component of the stress exceeds 0.8 dyn cm^{-2} in IH, in contrast to 0.4 dyn cm^{-2} in HR. (Note that this difference diminishes towards the equator only because of the blending of the IH stresses with HR which has been applied in this study.)

These strong differences between the stress climatologies demonstrated the important effect of the Beaufort equivalent particularly in the tropics. In both climatologies, westward stress at about 5°N ceases in August, defining the only location in the tropics where the difference between IH and HR becomes small.

The seasonality of the stresses and their differences are emphasized for 3 particular latitudes. Figure 5 displays the temporal variability at $\phi_1 = 52$°N, (maximum westerlies), $\phi_2 = 14$°N (maximum northeast trades) and $\phi_3 = 8$°N (6°N) which characterizes the annual cycle associated with the meridional shift of the ITCZ.

At 52°N, the amplitude of the annual cycle of westerly wind stress is reduced in IH, mainly due to the enhanced values during the period of weak stresses in summer. Maximum differences are about 0.25 dyn cm^{-2}, which represent a 38% change relative to HR. From January through March the zonal stresses in IH are smaller than in HR (by about 0.25 dyn cm^{-2} or 15%) as would be expected from the reduction of the drag coefficient. Additional differences, however, occur during fall (see also Fig. 4) where the IH wind stresses show a relative minimum in November. This minimum—which is not seen with HR—is a regional feature of the westerlies and is caused by a substantial decrease of directional steadiness of the wind from October to November (see Isemer and Hasse 1985) leading to reduced resultant wind vectors and, consequently, to reduced wind stresses in November. In December, the wind again blows more steadily increasing the resultant wind and the wind stress. The meridional component of the stress is smaller than the zonal one. Except for the first two months, there is a general tendency therefore for increased magnitudes in IH.

The second latitude displayed here, 14°N, represents the location of maximum easterly stress of the northeast trades. The climatologies show very similar seasonal cycles here, both for the zonal and meridional component. The IH stresses are simply shifted to higher magnitudes, by about 0.3 dyn cm^{-2} for the zonal, and 0.1–0.2 dyn cm^{-2} for the meridional component; there is no significant change in the amplitude of the annual cycle, however.

This is in marked contrast to latitudes south of $\sim$10°N which are directly affected by the annual migration of the ITCZ. For the zonal stress, the biggest seasonal cycle is near the latitude of the summer position of the ITCZ where this component nearly ceases. This is roughly the case at 8°N for both climatologies. The winter maximum of easterly stress is larger in IH by 0.3 dyn cm^{-2}, enhancing the amplitude of the annual cycle by nearly 50%. Biggest amplitudes in the variation of the meridional component are found at latitudes which are influenced in turn by the northeast and the southeast trades, i.e., between the equator and the northernmost extension of the ITCZ. In Fig. 5 the behavior at 6°N is displayed. In HR this stress component varies between -0.48 dyn cm^{-2} in winter to $+0.52$ in summer; with IH the numbers are -0.70 and $+0.77$. Again this means an increase of the annual amplitude by about 50%.

To conclude this section, we summarize the main features of the wind stress differences by Fig. 6 with the latitudinal dependence of the annual mean, zonally averaged components. Figures 6a and 6c show the zonal and meridional components, respectively, and Figs. 6b and 6d give the differences between IH and HR. The annual mean stresses of IH in the trade wind region are stronger by about 25% ($+0.3$ dyn cm^{-2} in the eastward and $+0.1$ dyn cm^{-2} in the southward component). Between 35° and 55°N, westerly stress in IH is reduced by about 0.07 dyn cm^{-2}, a relatively small percentage change. In this region the intensification of northward stress is more important.

4. Sverdrup transport

The curl of the wind stress is a central quantity for discussing the large-scale, wind-driven ocean circulation. Ekman theory relates $\mathrm{curl}_z(\vec{\tau}/f)$, where f is the Coriolis parameter, to the divergence of the wind-driven transport in the surface (Ekman) layer of the ocean. This is associated with a vertical velocity at the base of the Ekman layer which can be regarded as the forcing term of the interior flow.

It is easier, however, to interpret the implications of

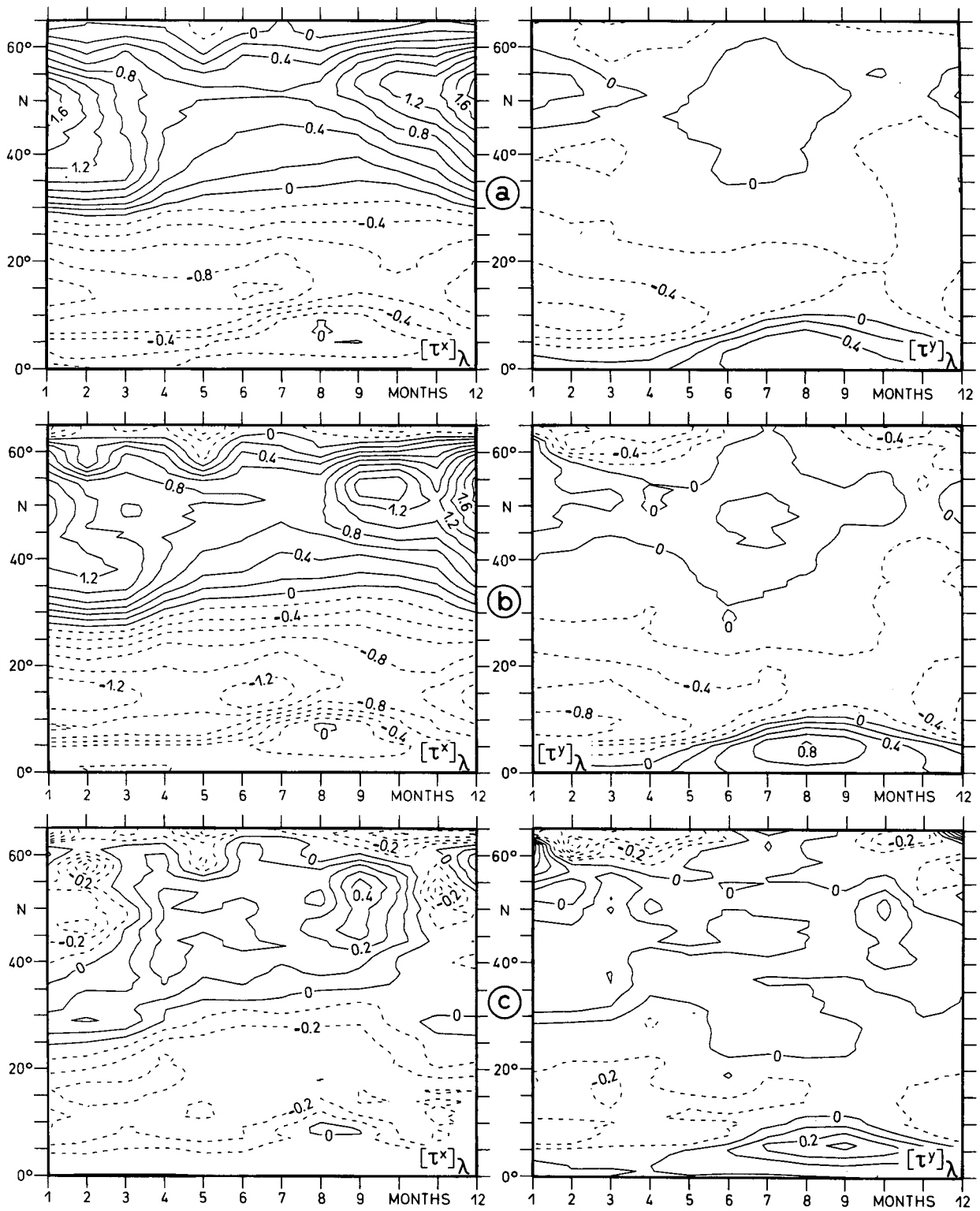

FIG. 4. Zonally averaged wind stress components, $[\tau^x]_\lambda$ in the left column, $[\tau^y]_\lambda$ in the right column, as functions of latitude and time. (a) HR, (b) IH, (c) IH minus HR, in dyn cm^{-2}.

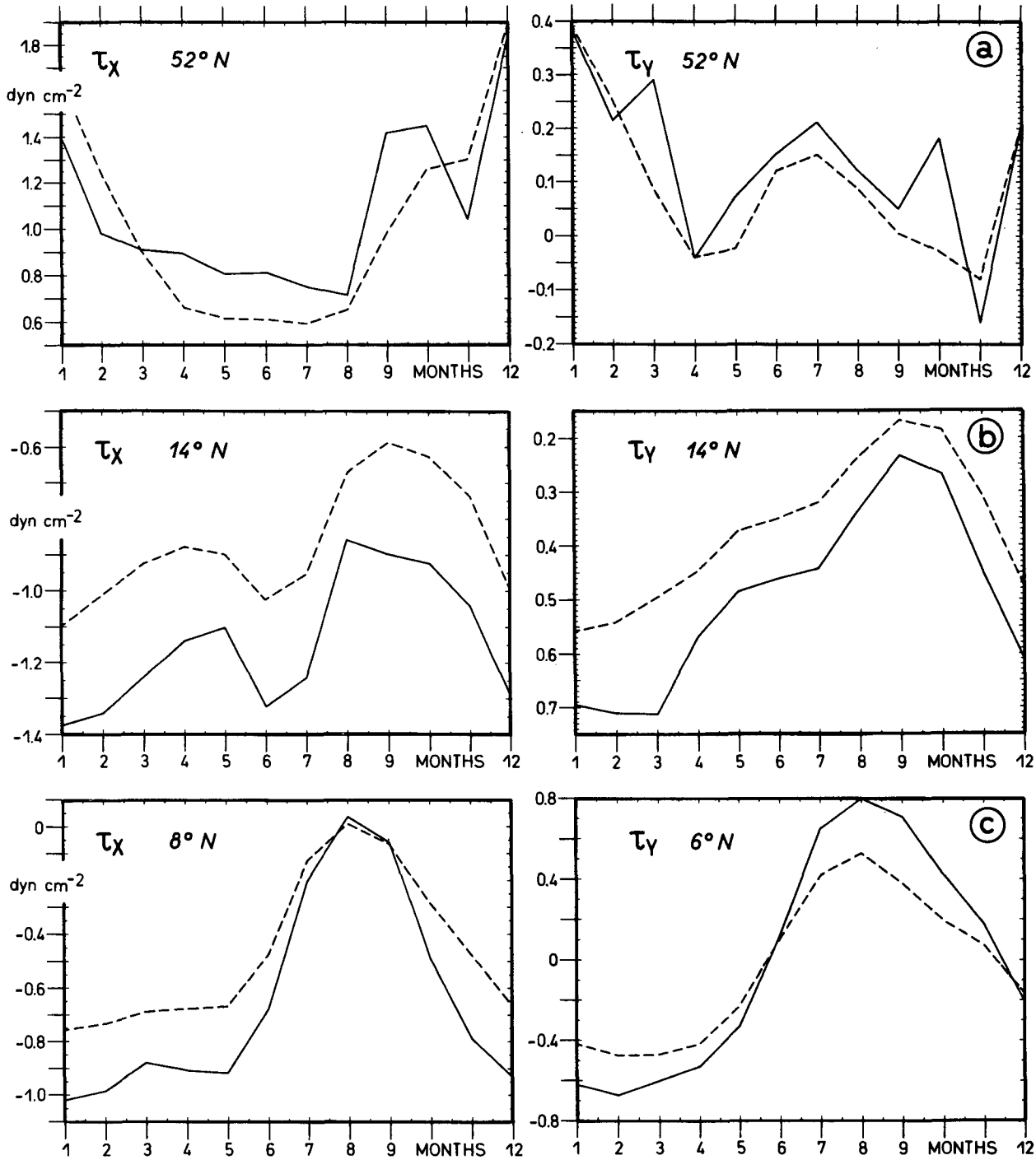

FIG. 5. Time dependence of the zonally averaged wind stress components at 52°N (a), 14°N (b), 8° and 6°N (c), for IH and HR (dashed).

the wind stress curl through the streamfunction ψ_S of the Sverdrup transport, obtained by integrating $\mathrm{curl}\vec{\tau}$ zonally across the basin

$$\psi_S(x) = -\int_{x_E}^{x} \frac{\mathrm{curl}_z(\vec{\tau})}{\beta}\, dx', \qquad (4)$$

where β is the meridional derivative of the Coriolis parameter. The integration starts at the eastern boundary x_E of the ocean basin, where the assumption is made that ψ_S vanishes. The calculation of $\mathrm{curl}\vec{\tau}$ was based on the wind stress fields given on the $1° \times 1°$-grid as discussed above.

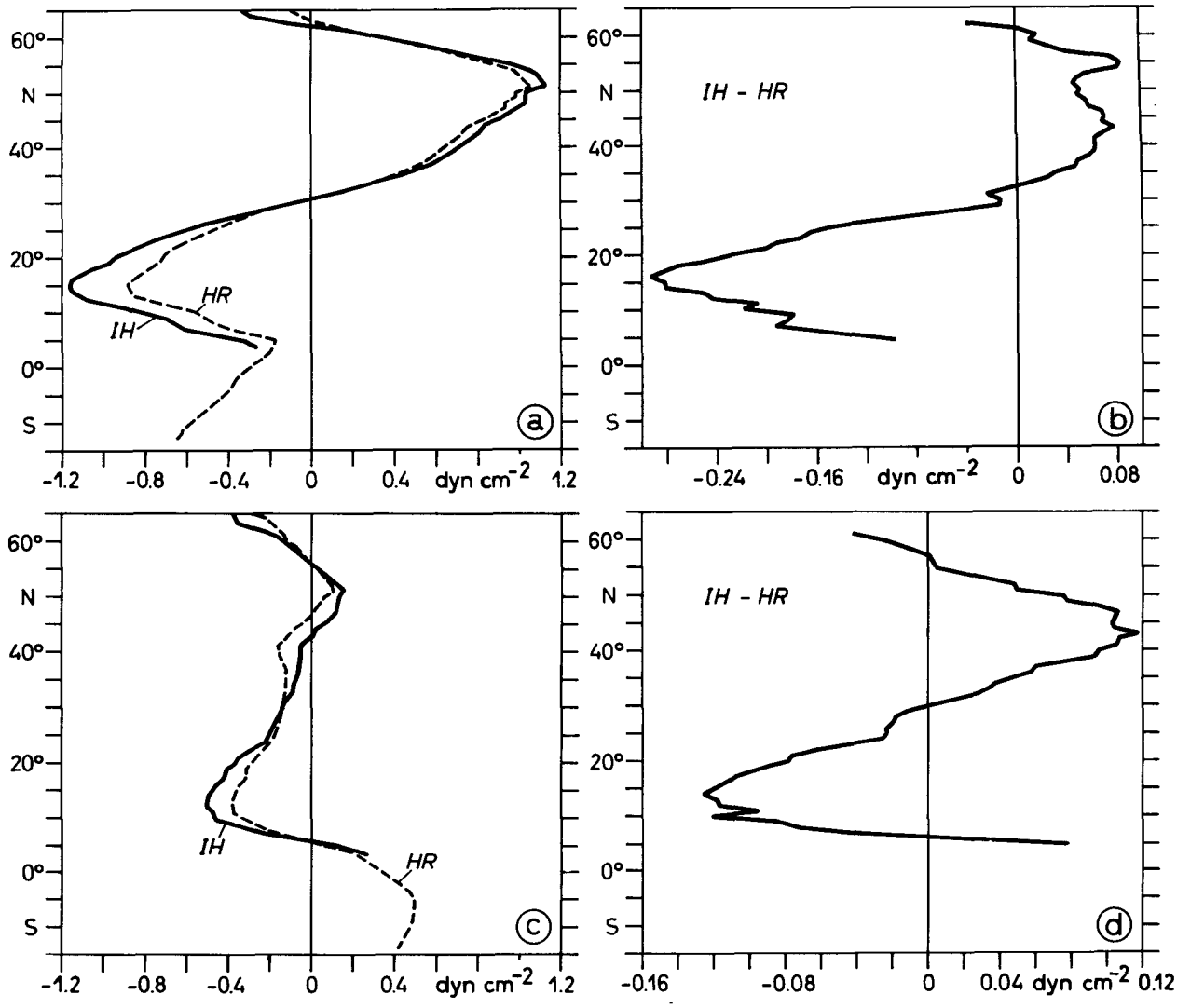

FIG. 6. Latitudinal dependence of the zonally averaged, annual mean wind stress components. (a) Zonal stress components of IH and HR (dashed); (b) zonal stress difference; (c) meridional stress components of IH and HR; (d) meridional stress difference.

Figure 7 shows the mass transport streamfunction ψ_S associated with the annual mean wind stress for both HR and IH. The outstanding feature of these fields is the anticyclonic circulation pattern in the subtropics, between the maximum of the westerlies at ~50°N and the maximum of the northeast trades at ~15°N. The IH fields lead to higher values of curl$\vec{\tau}$ and, subsequently, ψ_S in the subtropical gyre. Since curl$\vec{\tau}$ is mostly influenced by the meridional gradient of τ^x, the enhancement of ψ_S can be understood as a consequence of the substantially different values of τ^x in the northeast trades. The maximum values of the Sverdrup streamfunction are found near the western boundary at ~30°N.

In order to enable an easier comparison of the fields we display the values of ψ_S along the western boundary (i.e., along the dashed line indicated in Fig. 7), denoted by ψ_{SB}, as a function of latitude (Fig. 8). The representation reveals that throughout the subtropical gyre the transport is larger in the case of IH, especially in its southern part. Between 26°N and 28°N the IH transports exceed HR by more than 10 Sv.

Figure 6 indicates that south of the latitude of maximum easterly wind stress the meridional gradient of τ^x does not change very much between the climatologies. Accordingly, we find no significant changes in annual mean Sverdrup transport of the cyclonic gyre south of 15°N. We should expect, however, that the seasonal response of the cyclonic gyre to the monthly mean curl$\vec{\tau}$ fields becomes different because near the ITCZ strong differences occur between the seasonalities of the climatologies.

A problem with interpreting the seasonal response of the ocean circulation to monthly mean stresses is

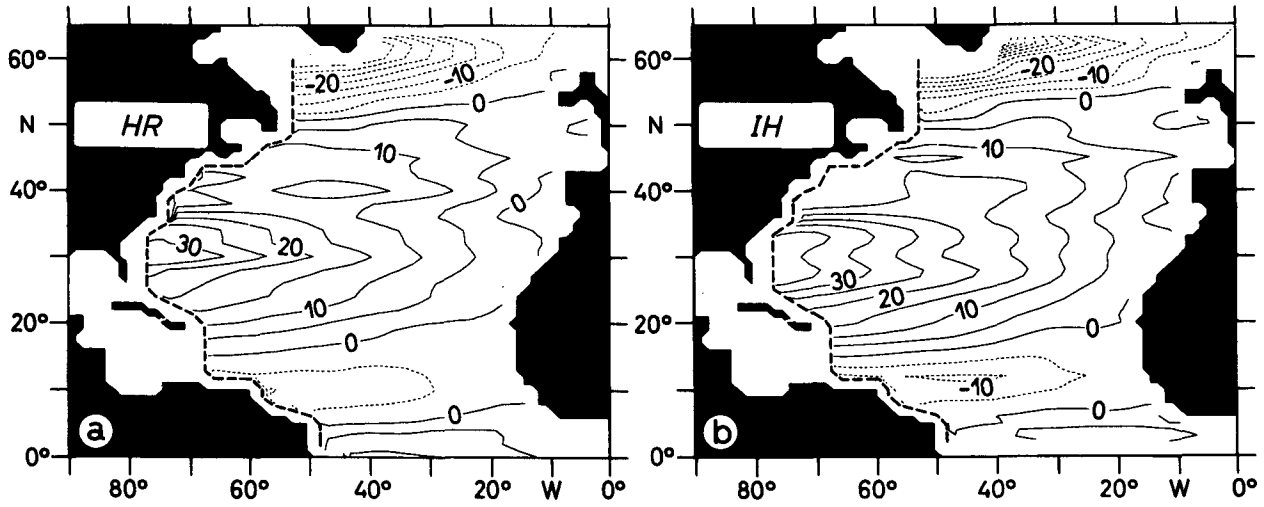

FIG. 7. Streamfunction Ψ_S of the annual mean Sverdrup volume transport. Contour interval 5 Sv (1 Sv $\equiv 10^6$ m^3 s^{-1}).

the inapplicability of the nontopographic Sverdrup relation. The balance between wind stress curl and meridional mass transport only applies to "long" time scales, i.e., long compared with the period of baroclinic Rossby waves. This time scale rapidly increases with latitude so that Eq. (4) is not valid for individual months or seasons, except for near-equatorial regions, maybe $\leq 10°$ latitude. Despite this fundamental difficulty we chose to display the seasonal cycle of ψ_S as a convenient integral measure of the seasonality of curl$\vec{\tau}$ over the ocean basin. Figure 9 displays ψ_{SB} as a function of latitude and time. In Fig. 10 the time dependence has been extracted for selected latitudes.

In the subpolar gyre, differences in the annual amplitude of ψ_{SB} are rather small, except for more intense fluctuations with shorter periods in IH. The amplitudes of the annual cycle are similar also in the northern portion of the subtropical gyre. An example is shown in Fig. 10a. At 32°N, IH (HR) gives a variation of ψ_{SB} between 48 Sv (50 Sv) in winter and 17 Sv (15 Sv) in summer. In a narrow band, centered at 30°N, there is a larger amplitude in HR due to a significantly stronger winter maximum than in IH.

Differences between the annual cycles of the curl$\vec{\tau}$ fields become more pronounced equatorward. It was noted already that in the southern part of the subtropical gyre the annual mean transport in IH is systematically stronger than in HR. Figure 10b shows that this tendency persists throughout the year. Since the differences between HR and IH are stronger in winter, the amplitude of the annual cycle also increases [at 24°N from 18 (HR) to 29 Sv (IH)].

Strong effects can be seen also in the amplitudes of the cyclonic gyre south of the trade wind maximum, and in the anticyclonic gyre south of the ITCZ. At 12°N (Fig. 10c) the summer maximum of ψ_{SB} increases from 23 Sv in HR to 34 Sv in IH; also, the summer maxima of the anticyclonic gyre at 6°N are 17 Sv (HR) and 24 Sv (IH), respectively (Fig. 10d).

Since the amplitude and phase of the oceanic re-

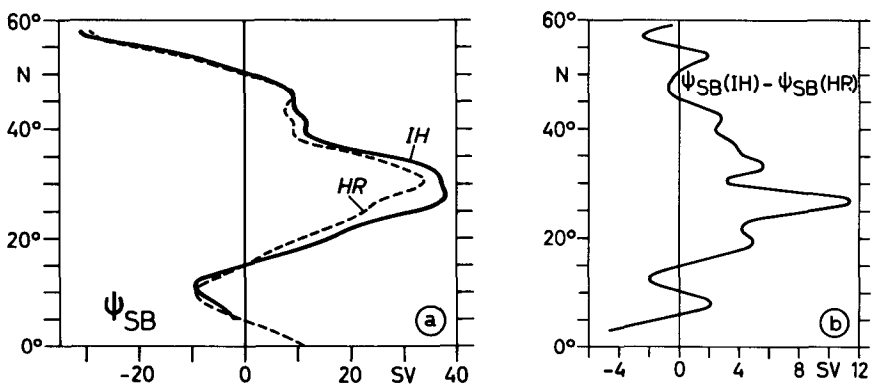

FIG. 8. Latitudinal dependence of the Sverdrup transport streamfunction along the western boundary (indicated by the dashed line in Fig. 7), Ψ_{SB}; (a) for HR and IH, (b) difference between IH and HR.

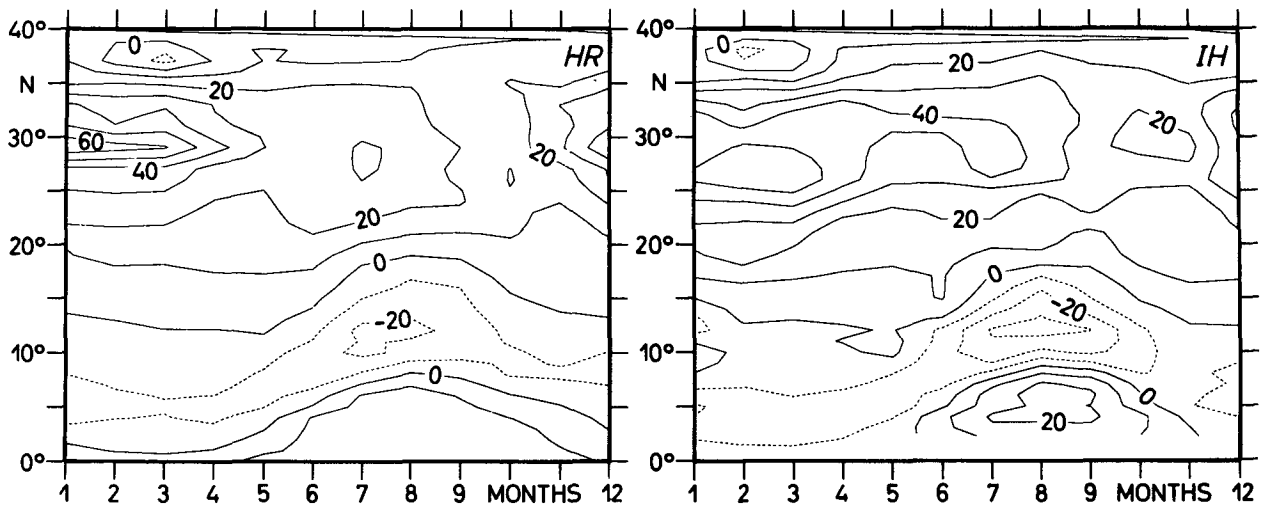

FIG. 9. Value of the Sverdrup transport streamfunction at the western boundary, Ψ_{SB}, as a function of latitude and time (in Sv).

sponse to monthly $\vec{\tau}$-fields cannot easily be inferred via the Sverdrup relation (4), we will conclude this section by presenting results of a sensitivity experiment with an eddy-resolving model of the North Atlantic circulation. The model configuration had been developed as a first step in a "community modeling effort" of the World Ocean Circulation Experiment. A discussion of the model and the first experiment performed at NCAR is given by Bryan and Holland (1989). In subsequent experiments the model is being used at IfM Kiel for studying the oceanic response to variable wind fields. In a first step we examined the sensitivity of the model circulation to forcing with different monthly mean wind stress climatologies, i.e., HR and IH. A detailed discussion of the experiments is presented elsewhere (Böning et al. 1990), it seemed appropriate, however, to include some aspects of the model predicted transports through the Straits of Florida here because they hint at the importance of the wind stress differences discussed above.

Figure 11a shows the annual cycle of the volume transport through Florida Straits. Though monthly mean forcing fields are applied, the model response contains flow variability from synoptic eddies to interannual variability. The dashed line represents the 5-year mean transport for the case that the model is forced by HR, and the heavy line gives the mean transport forced by IH. The stippling indicates the standard deviation from the 5-year mean value.

When using HR, the annual mean transport predicted by the model is 23.2 Sv. The annual range is rather small in this case, about 3.4 Sv. Both the mean transport and the amplitude of the annual cycle significantly increase when the model is forced by IH: the model then gives a mean of 29.1 Sv with an annual range of 6.3 Sv. A maximum of ~33 Sv is obtained in July, and a minimum of ~26 Sv in November. Figure 11b shows observationally derived, mean monthly transports through Florida Straits as given by Schott et al. (1988) (from current meter measurements) and Molinari et al. (1990) (a composite of various studies using dropsondes and PEGASUS profilers). The annual cycle is quite asymmetric, with a broad summer maximum, and a pronounced minimum in fall. Probably the most stable feature of the observations is the rapid drop from July–August to October–November. The annual range, i.e., the difference between the summer maximum and the fall minimum, has been used repeatedly as a test of circulation models (e.g., AC; GG; Schott et al. 1988). It can be seen that the model is in much better agreement with the observational evidence, both with respect to the annual mean and the annual range, when it is forced by IH.

Obviously, model results can be influenced by a whole suite of parameterization and parameter choices. In principle, there remains an uncertainty therefore with respect to the dependence of the transport to model resolution, to details of the topographic structure, or to friction coefficients. It is interesting to note, however, that amplitude and phase of the annual cycle obtained with HR forcing in the present, high-resolution model is very similar to results obtained by Anderson and Corry (1985), and Greatbatch and Goulding (1989) with coarser models, using idealized basin geometries. The similarity of the model solutions, when forced by the same wind stress, indicates a rather robust nature of the transport variation in the straits. The range of the annual variation seems to be more sensitive to the wind forcing than to details of the model configuration.

5. Conclusions

The calculation of wind stress fields over the ocean based on historical records of marine observations im-

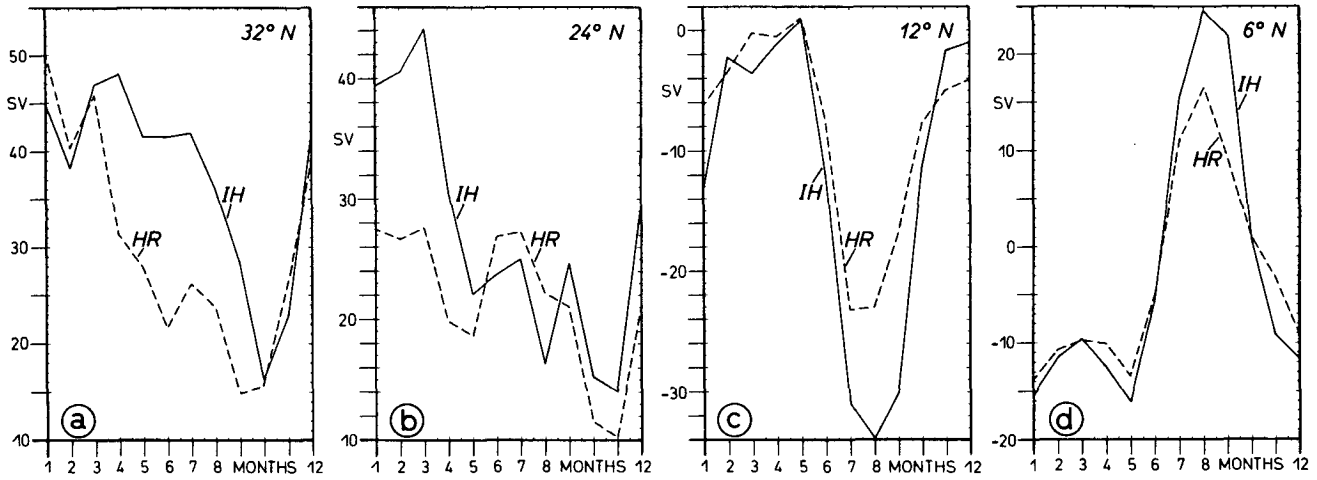

FIG. 10. Time dependence of Ψ_{SB} (in Sv) at (a) 32°N, (b) 24°N, (c) 12°N, (d) 6°N.

plies several problems. Apart from a poor data density in many regions resulting in the need to strong spatial interpolation, the most significant uncertainties arise from the estimation of wind speed based on ship observation at sea, and the parameterization of the surface momentum flux by a bulk aerodynamic formula. Whereas the critical role of the surface drag coefficient and its dependence on wind speed and atmospheric stability had, in principle, been recognized for a long time, this seems not to be the case with respect to the Beaufort equivalent scale. Estimates of the uncertainty in calculating wind stress have been based previously on the standard error associated with averaging individual observations (Hellerman and Rosenstein 1983), or a plausible uncertainty of the neutral stability form of c_D (Harrison 1989).

Harrison's use of the Large and Pond (1981) form of c_D instead of the form adopted by Bunker (1976) caused differences in the resulting wind stresses, which generally significantly exceeded the uncertainty estimates of HR. In their calculation of surface fluxes for the North Atlantic Ocean, IH used a form of c_D rather similar to the one preferred by Large and Pond, but directed attention also on the Beaufort equivalent scale. Their work showed that using revised Beaufort equivalents as recommended by WMO for scientific purposes significantly increased the estimated values of $\vec{\tau}$ in many parts of the ocean basin.

Here we presented an evaluation of the IH-climatology in comparison with the widely used wind stress climatology of HR. It could be shown that in most regions the revision of the Beaufort equivalents has a stronger effect on $\vec{\tau}$ than the reduction of the drag coefficient. The influence of the correction factor for the wind speed is most pronounced in subtropical and equatorial regions; here the stress estimates of IH are significantly increased relative to HR. Since the effect due to reducing c_D and the effect due to revising the wind climatologies counteract each other, even bigger differences result when the IH values are compared with those of Harrison (1989) who altered one of those factors (c_D) alone. Whereas the magnitude of the annually averaged, zonal stresses of HR in the trade wind region are lowered by more than 0.2 dyn cm^{-2} when using the revised c_D (Harrison 1989), IH get an increase relative to HR by 0.3 dyn cm^{-2}. Thus there is nearly a 100% difference between the stress values of Harrison and IH in these regions.

The surface momentum flux is the most important factor for forcing the circulation in the upper layers of the ocean. Numerical models of large-scale ocean circulation have to rely on wind stress estimates based on surface marine observations. The strong differences between recently prepared monthly mean wind stress climatologies demonstrate the need for intensifying efforts on this aspect of atmosphere–ocean interaction. How can the performance of ocean circulation models be improved when there is a factor of 2 uncertainty in the forcing fields?

One way of reducing the existing uncertainties in calculating $\vec{\tau}$ could be the use of an inverse approach to adjust the coefficients of the parameterizations (within their error limits) by comparing predictions of wind-driven oceanic transports with direct observations. An inverse technique had been applied by IH (see also Isemer et al. 1989) with respect to the surface heat flux. In case of $\vec{\tau}$, however, it is complicated in that no simple relation exists between the time-dependent wind stress over the ocean basin and the western boundary current transport. A particularly useful constraint could be given by the transport through Florida Straits which had been observed extensively in recent years (e.g., Schott et al. 1988). A prediction of wind generated transports has to rely, however, on quite sophisticated numerical models which must be able to resolve both the North Atlantic basin and the bathymetry of the narrow western passages.

The results obtained with the high resolution Atlantic

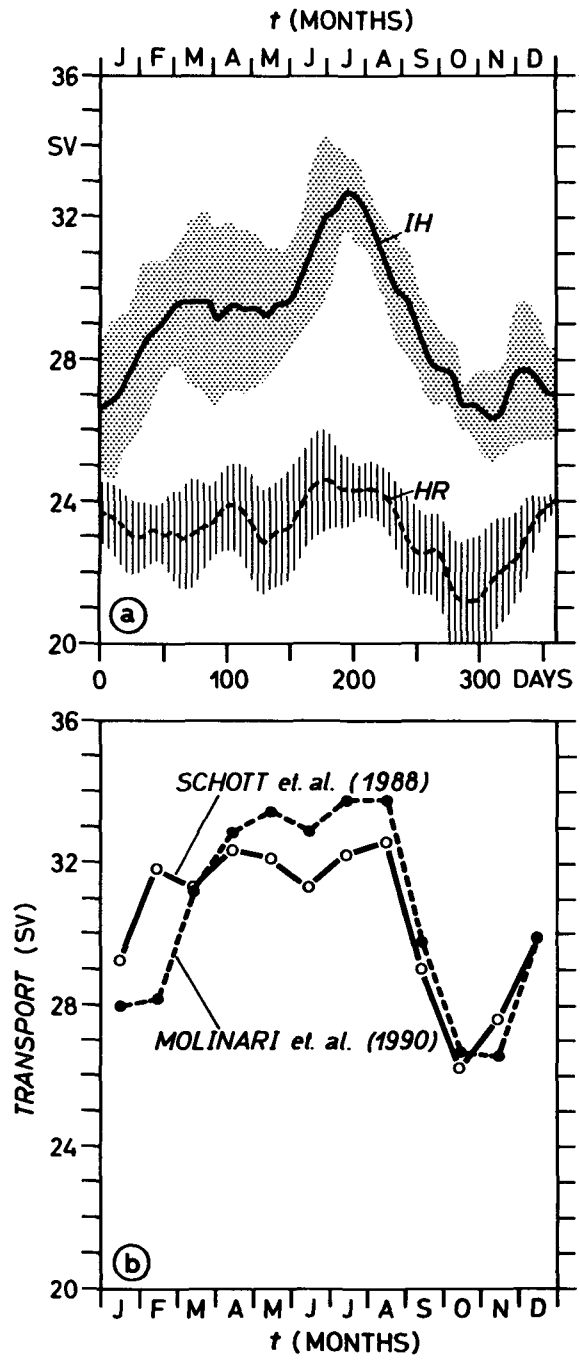

FIG. 11. Annual cycle of the volume transport through Florida Straits. (a) Results of the eddy-resolving circulation model, forced with HR and IH. Displayed are the mean cycles over a 5-year integration period; the stippling indicates the standard deviation due to the interannual variability of the model response. (b) Transport estimates from Schott et al. (1988), based on current meter moorings in the time interval from April 1982 to June 1984, and from Molinari et al. (1990), a composite of various observations with dropsondes and velocity profilers.

model as shown in Fig. 11 indicate a much better agreement with the observed annual cycle of Florida Straits transport when the circulation is forced by the IH climatology instead of HR. It is obvious that using the climatology of Harrison would lower the predicted transport even more than HR. Clearly, results like these can be biased by possible errors in the model used. It would seem to be important therefore to repeat such sensitivity experiments with different models. It also appears important that ocean modelers are aware of the uncertainties and the differences between existing wind stress climatologies.

From a meteorological point of view the IH climatology has to be considered as most reliable because wind statistics *and* parameterization techniques are based on newer experimental evidence while both BU and HR are based on older evidence with respect to c_D, and the wind stress climatology of Harrison (1989) apparently considered only the revision of one factor (c_D) alone. The IH climatology, as shown here, finds additional support by independent, oceanographic evidence.

Acknowledgments. We thank F. Bryan and W. Holland for providing the CME code and data fields, and their valuable assistance in implementing the model at the CRAY X-MP of Kiel University. We also wish to acknowledge the participation of R. Budich in the numerical integrations, and we thank R. Gerdes and J. Kielmann for their efforts at improving computational efficiency. This study is supported by the Deutsche Forschungsgemeinschaft, Sonderforschungsbereich 133.

REFERENCES

Anderson, D. L. T., and R. A. Corry, 1985: Seasonal transport variation in the Florida Straits: a model study. *J. Phys. Oceanogr.*, **15,** 773–786.

Böning, C. W., R. Döscher and R. G. Budich, 1990: Seasonal transport variation in the western subtropical North Atlantic: experiments with an eddy-resolving model. *J. Phys. Oceanogr.* submitted.

Blanc, T. V., 1985: Variation of bulk-derived surface flux, stability, and roughness results due to the use of different transfer coefficient schemes. *J. Phys. Oceanogr.*, **15,** 650–669.

Bryan, F. O., and W. R. Holland, 1989: A high-resolution simulation of the wind- and thermohaline driven circulation in the North Atlantic Ocean. *Parameterization of Small-Scale Processes, Proc. 'Aha Huliko'a, Hawaiian Winter Workshop,* Manoa, University of Hawaii at Manoa, 99–115.

Bunker, A. F., 1976: Computations of surface energy flux and annual air–sea interaction cycles of the North Atlantic Ocean. *Mon. Wea. Rev.*, **104,** 1127–1140.

Cardone, V. J., J. G. Greenwood and M. A. Cane, 1990: On trends in historical marine wind data. *J. Climate,* **3,** 113–127.

Coads, 1985: *Comprehensive Ocean–Atmosphere DataSet, Release 1.*

Deardorff, J. W., 1968: Dependence of air–sea transfer coefficients on bulk stability. *J. Geophys. Res.*, **73,** 2549–2557.

Greatbatch, R. J., and A. Goulding, 1989: Seasonal variations in a linear barotropic model of the North Atlantic driven by the Hellerman and Rosenstein wind stress field. *J. Phys. Oceanogr.*, **19,** 572–595.

Harrison, D. E., 1989: On climatological monthly mean wind stress and wind stress curl fields over the world ocean. *J. Climate,* **2,** 57–70.

Hasse, L., M. Grünewald, J. Wucknitz, M. Dunkel and D. Schriever, 1978: Profile-derived turbulent fluxes in the surface layer under disturbed and undisturbed conditions during GATE. "Meteor" Forschungsergeb. *Reihe,* **B,13,** 24–40.

Hellerman, S., 1967: An updated estimate of the wind stress in the World Ocean. *Mon. Wea. Rev.,* **95,** 607–611.

——, and M. Rosenstein, 1983: Normal monthly wind stress over the World Ocean with error estimates. *J. Phys. Oceanogr.,* **13,** 1093–1104.

Isemer, H.-J., and L. Hasse, 1985: The Bunker climate atlas of the North Atlantic Ocean. Vol. 1 *Observations,* Springer-Verlag, 218 pp.

——, and ——, 1987: The Bunker climate atlas of the North Atlantic Ocean. Vol. 2 *Air—Sea Interactions,* Springer-Verlag, 256 pp.

——, and ——, 1990: Application of a scientific Beaufort scale: Effects on North Atlantic Ocean wind statistics and climatological air–sea flux estimates. *J. Climate.*

——, J. Willebrand and L. Hasse, 1989: Fine adjustment of large-scale air–sea energy flux parameterizations by direct estimates of ocean heat transport. *J. Climate,* **2,** 1173–1184.

Kaufeld, L., 1981: The development of a new Beaufort equivalent scale. *Meteorol. Rundsch.,* **34,** 17–23.

Large, W. G., and S. Pond, 1981: Open ocean momentum flux measurements in moderate to strong winds. *J. Phys. Oceanogr.,* **11,** 324–336.

Molinari, R. L., E. Johns and J. F. Festa, 1990: The annual cycle of meridional heat flux in the Atlantic Ocean at 26.5°N. *J. Phys. Oceanogr.,* **20,** 476–482.

Oberhuber, J. M., 1988: An atlas based on the "COADS" dataset: the budgets of heat, buoyancy, and turbulent kinetic energy at the surface of the global ocean. Max-Planck-Institut für Meteorologie, Hamburg, F.R.G., Report No. 15, 20 pp. (176 charts)

Quayle, R. G., 1980: Climatic comparisons of estimated and measured wind from ships. *J. Appl. Meteor.,* **19,** 142–156.

Schott, F. A., T. N. Lee and R. Zantopp, 1988: Variability of structure and transport of the Florida Current in the period range from days to seasonal. *J. Phys. Oceanogr.,* **18,** 1209–1230.

Scoggins, J. R., and C. N. R. Mooers, 1989: Workshop on Atmospheric Forcing of Ocean Circulation. *Bull. Amer. Meteor. Soc.,* **69,** 1349–1353.

Smith, S. D., 1980: Wind stress and heat flux over the ocean in gale force winds. *J. Phys. Oceanogr.,* **10,** 709–726.

World Meteorological Organization, 1970: Reports on marine scientific affairs. Rep. No. 3. The Beaufort scale of wind force. WMO, Geneva, 22 pp.